IOPscience iopscience.iop.org

Home Search Collections Journals About Contact us My IOPscience

Calculation of spin and orbital magnetizations in Fe slab systems at finite temperature

This article has been downloaded from IOPscience. Please scroll down to see the full text article.

2010 J. Phys.: Condens. Matter 22 056001

(http://iopscience.iop.org/0953-8984/22/5/056001)

View the table of contents for this issue, or go to the journal homepage for more

Download details:
IP Address: 129.252.86.83
The article was downloaded on 30/05/2010 at 07:03

Please note that terms and conditions apply.

IOP Publishing Journal of Physics: Condensed Matter

J. Phys.: Condens. Matter **22** (2010) 056001 (11pp) doi:10.1088/0953-8984/22/5/056001

Calculation of spin and orbital magnetizations in Fe slab systems at finite temperature

R Garibay-Alonso[1], M Reyes-Reyes[2], Efraín Urrutia-Bañuelos[3] and R López-Sandoval[4]

[1] Facultad de Ciencias Físico Matemáticas, Universidad Autónoma de Coahuila, Conjunto Universitario Camporredondo, Edificio 'D', 25000 Saltillo, Mexico
[2] Instituto de Investigación en Comunicación Optica, Universidad Autónoma de San Luis Potosí, Alvaro Obregón 64, San Luis Potosí, Mexico
[3] Departamento de Investigación en Física, Universidad de Sonora, Apartado Postal 5-088, Hermosillo, Sonora 83190, Mexico
[4] Instituto Potosino de Investigación Científica y Tecnológica, Camino a la presa San José 2055, CP 78216, San Luis Potosí, Mexico

Received 2 October 2009, in final form 17 November 2009
Published 15 January 2010
Online at stacks.iop.org/JPhysCM/22/056001

Abstract
The temperature dependence of spin and orbital local magnetizations is theoretically determined for the non-bulk atomic region of (001) and (110) Fe slab systems. A d band Hamiltonian, including spin–orbit coupling terms, was used to model the slabs, which were emulated by using Fe films of sufficient thickness to reach a bulk behavior at their most inner atomic layers. The temperature effects were considered within the static approximation and a simple mean field theory was used to integrate the local magnetic moment and charge thermal fluctuations. The results reflect a clear interplay between electronic itinerancy and the local atomic environment and they can be physically interpreted from the local small charge transfers occurring in the superficial region of the slabs. For recovering the experimental behavior on the results for the (001) slab system, the geometrical relaxations at its non-bulk atomic layers and a d band filling variation are required. A study on the magnetic anisotropy aspects in the superficial region of the slabs is additionally performed by analyzing the results for the orbital local magnetization calculated along two different magnetization directions in both slab systems.

1. Introduction

The local atomic environment and temperature dependence of the magnetic properties in the superficial region of a macroscopic transition metal (TM) magnetic system play a fundamental role in experimental situations where these systems are in physical interaction with other nanostructured magnetic systems such as clusters or thin films [1]. As it is known, a full characterization of this dependence can help to determine the general character of the mentioned physical interaction and also to know how it will affect, in turn, the magnetic properties of the whole interacting system. On the other hand, the theoretical study of the finite temperature magnetic properties in the superficial region of a TM magnetic material gives the opportunity to explore and observe in a detailed way the magnetism of a system with reduced dimensionality [2–7]. This kind of study could help in obtaining new insights in the development of novel materials for technological purposes.

In recent years [5], the use of several experimental techniques, such as spin-resolved secondary electron emission [2] or spin-resolved photo-emission [3], have been used to determine, with atomic resolution, the temperature dependence of the magnetization in the superficial region of TM magnetic systems. Unfortunately, these techniques average over several adjacent atomic layers giving the same bulk-like behavior in the temperature dependence of the magnetization on and near the surface of the systems. However, other relatively recent experimental approaches using photo-emission dichroism or spin-polarized electron capture techniques [4, 5] have proven

 © 2010 IOP Publishing Ltd Printed in the UK

to be successful in obtaining the desired atomic resolution. In particular, Pfandzelter and Potthoff [5] measured the temperature dependence of the magnetization in the superficial region of a macroscopic Fe (001) slab with a one-monolayer resolution and obtained a linear trend in the most superficial atomic layers. In addition, they studied the problem in a theoretical way by using a Heisenberg Hamiltonian in the mean field approximation and found that their calculations give a good description of the local magnetization at finite temperature. In this work, we are extending the theoretical part of the work of Pfandzelter and Potthoff to determine, in the framework of an itinerant electron model, the spin and orbital contributions to the total magnetization in the system. To the best of our knowledge, this is the first time that the temperature dependence of the orbital magnetization has been theoretically determined for a TM system with effects of reduced dimensionality. Besides this relevance, some conclusions concerning the magnetic anisotropy aspects in the superficial region of the system are also inferred from the results for the orbital magnetic polarization calculated along several magnetization directions. The research of the electronic itinerancy effects at finite temperature on the magnetism of the system in its superficial region is highly desirable because of the abrupt change in the local atomic environment occurring at its boundary.

Although many theoretical calculations involving spin–orbit coupling (SOC) effects in TM magnetic systems are already found in the literature for zero temperature [8, 9] (ground state), for finite temperatures, this kind of calculation is scarce because of the difficulties introduced by many-body aspects [10]. When we try to obtain reliable results for finite temperatures, one arrives at the problem of implementing and/or developing theories which consider the relevant physical aspects related to the properties of the systems under study. In the case of itinerant electron magnetic systems with reduced dimensionality, the electronic itinerancy and the SOC interaction (responsible for the orbital polarization in a TM magnetic system) must be taken into account by the theory in order to obtain a proper dependence on the local atomic environment in the results. In the literature, one can find several different approaches for calculating the magnetic properties of itinerant electron magnetic systems which take (or could take) into account these two physical aspects. One can mention, for instance, the case of the static Hartree–Fock and Gutzwiller approximations, dynamical mean field theory (DMFT) applied on Hubbard-like Hamiltonians and spin fluctuation theories (SFT). Some of these approaches, such as the static Hartree–Fock and Gutzwiller [11] approximations, were originally developed for working only at zero temperature and their extensions to the finite temperature region are considered as equivalent to the SFT approaches. Some others, such as the DMFT [12] implemented on Hubbard-like Hamiltonians, are approaches which handle in a reliable way the finite temperature magnetic properties related to electron correlation effects. However, the current implementations of the DMFT for the systems of our interest are based on mean field Monte Carlo calculations which could with difficulty quantify the effects of the SOC interaction on the finite temperature magnetic properties, due to the relatively small intensity of the SOC interaction. Moreover, these implementations have been performed only, to the best of our knowledge, for the bulk cases of transition metal ferromagnetic systems and they have shown that the considered electron correlation effects do not play a very important role on some magnetic properties such as the Curie temperature and the qualitative functional dependence of the magnetization with temperature. On the other hand, the SFT [13–15] approaches are methods based on a decoupling of the spin and charge fluctuation transitions from the electronic hopping transitions on the basis of characteristic times. These approaches have been implemented on several models based on Hubbard, spd band and *ab initio* Hamiltonians. The success of the different implementations depends on the physical characteristic of the Hamiltonian model and mean field approach used for the specific implementation. In this work, we use a previously implemented finite temperature mean field SFT theory [14, 15], which considers the local atomic environment dependence of the electronic structure of a TM magnetic system and includes, for the first time, the SOC effects in a non-perturbative way. This theory is based in the use of a d band Hamiltonian and handles the finite temperature effects within the static approximation. In our approximation, the local fluctuations of the charge and magnetic moments originated by temperature effects are integrated into an effective medium by a simple mean field approach, which allows us to perform the calculations in feasible computational times. The Fe slabs are modeled by employing Fe films of a thickness sufficient to obtain, in a general way, the bulk behavior at their inner atomic layers.

The organization of the paper is as follows. In section 2, the theory used for the calculations is presented. In section 3, the local spin and orbital magnetization results are shown and discussed by analyzing their dependence on the local atomic environment of the system in question. Some magnetic anisotropy aspects, derived from the results for the orbital magnetization calculated along two different magnetization directions on the slabs, are also discussed in this section. Finally, section 4 summarizes the main conclusions of this work, indicating goals, limitations and some possible extensions.

2. Theory

To model the itinerant magnetism and the orbital polarization of a TM magnetic system we use the d band Hamiltonian [16]. This model is known from the literature to correctly describe the dependence of several magnetic properties (e.g. spin and orbital local moments and anisotropy energies) on the atomic local environment of transition metal systems with the effects of reduced dimensionality at zero temperature (see for example [8, 9]). The model is constructed on the basis that the magnetic properties of these systems can be described with electrons occupying quantum states with an atomically localized nature, which are constructed by atomic d orbital states and form d narrow energy bands on the system. The localized nature of the atomic d orbital states leads to

three important facts, an atomically localized character of the d electron–electron Coulomb interaction, a non-strong dependence of this Coulomb interaction on the local atomic environment and a relatively low hybridization of the narrow d band with the conduction sp bands of the systems. The effects of considering non-local d Coulomb interactions and/or hybridization effects with sp bands are generally small for zero temperature (they are of relative importance for zero temperature only for transition metal systems with an almost filled d band), as it can be consulted in [17]. The model is defined by

$$\hat{H} = \hat{H}_0 + \hat{H}_I + \hat{H}_{\mathrm{SOC}}, \tag{1}$$

where the first term

$$\hat{H}_0 = \sum_{l,\alpha,\sigma} \varepsilon_l^0 \hat{n}_{l\alpha\sigma} + \sum_{\substack{l\neq q \\ \alpha,\beta,\sigma}} t_{lq}^{\alpha\beta} \hat{c}_{l\alpha\sigma}^{\dagger} \hat{c}_{q\beta\sigma} \tag{2}$$

describes the one electron electronic structure of the valence d electrons in the tight-binding approximation. $\hat{c}_{l\alpha\sigma}^{\dagger}$ ($\hat{c}_{l\alpha\sigma}$) refers to the creation (annihilation) operator of an electron with spin σ at the atomic orbital α of atom l ($\alpha \equiv xy, yz, zx, x^2-y^2$, and $3z^2 - r^2$) and $\hat{n}_{l\alpha\sigma} = \hat{c}_{l\alpha\sigma}^{\dagger}\hat{c}_{l\alpha\sigma}$ is the electron number operator at the same atom. ε_l^0 is the bare d-level energy of an electron occupying the isolated atom and $t_{lq}^{\alpha\beta}$ are the hopping integrals between atoms l and q. The second term

$$\begin{aligned}\hat{H}_I &= \tfrac{1}{2}{\sum_{\substack{l,\alpha,\beta \\ \sigma,\sigma'}}}' U_{\sigma\sigma'} \hat{n}_{l\alpha\sigma}\hat{n}_{l\beta\sigma'} \\ &= \tfrac{1}{2}\sum_l (U\hat{N}_l^2 - 2J\hat{S}_{lz}^2 - (U - J/2)\hat{N}_l)\end{aligned} \tag{3}$$

takes into account the interactions among electrons by an intra-atomic Hubbard-like model. The Coulomb repulsions between electrons of spin σ and σ' are denoted by $U_{\sigma\sigma'}$. $U = (U_{\uparrow\downarrow} + U_{\uparrow\uparrow})/2$ represents the average direct Coulomb integral and $J = U_{\uparrow\downarrow} - U_{\uparrow\uparrow}$ the average exchange integral. $\hat{N}_l = \sum_{\alpha\sigma} \hat{n}_{l\alpha\sigma}$ is the total number operator at atom l and $\hat{S}_{lz} = (1/2)\sum_{\alpha}(\hat{n}_{l\alpha\uparrow} - \hat{n}_{l\alpha\downarrow})$ is the z component of the total spin operator at the same atom. Note that terms of the form $\hat{H}_{xy} = -\sum_{l,\alpha,\beta} J_{\alpha\beta}(\hat{S}_{l\alpha}^{+}\hat{S}_{l\beta}^{-} + \hat{S}_{l\beta}^{-}\hat{S}_{l\alpha}^{+})$, which represent transversal-spin-like interactions, have been dropped in equation (3). However, this is not expected to be a serious qualitative limitation in the present work, since we are interested in studying the effects of spin fluctuations on broken-symmetry ferromagnetic ground states. The third term

$$\hat{H}_{\mathrm{SOC}} = \xi_{\mathrm{SOC}} \sum_{l,m\sigma,m'\sigma'} (\vec{L}\cdot\vec{S})_{m\sigma,m'\sigma'} \hat{C}_{lm\sigma}^{\dagger}\hat{C}_{lm'\sigma'} \tag{4}$$

models the SOC interaction, where ξ_{SOC} is the SOC parameter and $\hat{C}_{lm\sigma}^{\dagger}$ ($\hat{C}_{lm\sigma}$) is the creation (annihilation) operator for an electron with spin σ at the spherical harmonic orbital m of atom l ($m = -2, -1, 0, 1, 2$). The SOC interaction magnetically reveals the structural anisotropy of a TM system and generates the biggest part of the total amount of its orbital polarization. Notice that the creation and annihilation operators used for expressing $\hat{H}_{\mathrm{SOC}}$ are different from those used for expressing the rest of the Hamiltonian terms in equations (1)–(3). In practice, only one kind of these operators is used when we are realizing the calculations and this depends on the physical quantities involved. The transformation from one kind of operator to another is performed following the canonical second quantization rules [18], which in this case involve the known relationship between atomic d-orbitals and spherical harmonics.

Within the model described above, the magnetic properties of a TM system at finite temperature can be determined by applying a grand canonical version of the functional-integral formalism implemented in [19] and [20] for the study of 3d TM clusters. This formalism is a variant of the original one developed by Hubbard and Hasegawa for studying periodic solids [13]. In the referenced formalism, the quadratic terms in equation (3) are linearized inside the partition function by means of a two-field Hubbard–Stratonovich transformation and, straight afterward, the spin and charge local fluctuations are decoupled from the relatively faster electronic hopping transitions by applying the static approximation [21]. After that, the system appears as formed by local charge and exchange fields fluctuating in an independent way and, by using the fact that $J \ll U$, the thermal fluctuations of the local charge fields are partially neglected by setting these fields equal to their local-exchange-field-dependent saddle-point values. This focuses the theory on the magnetic aspects of a system and leads to a self-consistent determination of the charge distribution for each configuration of the local exchange fields $\vec{\xi} = (\xi_1, \xi_2, \xi_3, \ldots)$. In a brief way, we have for the grand canonical case

$$Z \propto \int \mathrm{d}\vec{\xi}\, \tilde{Z}'(\vec{\xi}), \tag{5}$$

where

$$\begin{aligned}Z'(\vec{\xi}) &= \exp\{-\beta F(\vec{\xi})\} \\ &= \exp\left\{\frac{\beta}{2}\sum_l \left[U\nu_l^2 - \frac{J}{2}\xi_l^2\right]\right\} \mathrm{Tr}[\exp\{-\beta(\hat{H}' - \mu\hat{N})\}].\end{aligned} \tag{6}$$

In this equation,

$$\hat{H}' = \hat{H}_0 + \hat{H}_{\mathrm{SOC}} + \sum_{l\alpha\sigma}(U\nu_l - \sigma J/2\xi_l)\hat{n}_{l\alpha\sigma} \tag{7}$$

is the Hamiltonian associated to the exchange fluctuations of $\vec{\xi}$, including the SOC interaction in a full way and with the bare d-energy level redefined as $\varepsilon_l^0 \equiv \varepsilon_l^0 - (U - J/2)/2$. The quantity $F(\vec{\xi})$ in equation (6) represents a free energy associated to the exchange field configuration $\vec{\xi}$. The self-consistent saddle-point values

$$\nu_l = \langle \hat{N}_l \rangle_{\vec{\xi}}' \tag{8}$$

are calculated by taking averages at temperature T in the one electron states (this is indicated by the quote on the average symbol). The thermodynamic properties can be obtained by averaging over all possible $\vec{\xi}$ with $\exp\{-\beta F(\vec{\xi})\}$ as the weighting factor. For example, the local spin magnetization for the z direction at the atom l can be expressed as

$$\begin{aligned}M_{lz}(T) &= -\frac{\mu_{\mathrm{B}}}{Z}\int \mathrm{d}\vec{\xi}\, 2\langle \hat{S}_{lz}\rangle_{\vec{\xi}}' \mathrm{e}^{-\beta F'(\vec{\xi})} \\ &= -\frac{\mu_{\mathrm{B}}}{Z}\int \mathrm{d}\vec{\xi}\, \xi_l \mathrm{e}^{-\beta F'(\vec{\xi})},\end{aligned} \tag{9}$$

where μ_B is the Bohr magneton. Analogous relations to equation (9) exist for the local orbital magnetization and local charge. For instance, the local orbital magnetization for the z direction can be calculated as

$$L_{lz}(T) = -\frac{\mu_B}{Z}\int \mathrm{d}\vec{\xi}\,\langle \hat{L}_{lz}\rangle'_{\vec{\xi}} \mathrm{e}^{-\beta F'(\vec{\xi})}. \tag{10}$$

To perform the necessary statistical averages on the exchange field values, we use a simple mean field approach which consists in creating an effective medium characterized by an average of these fields [22]. The effective medium is defined by its associated effective Hamiltonian $\hat{H}_{\mathrm{eff}} = \langle \hat{H}' \rangle$, which depends in a self-consistent way on $\langle \nu_l \rangle$ and $\langle \xi_l \rangle$. The average values of the local charge and exchange fields are calculated by fluctuating the ξ_l field of a representative site immersed into the effective medium. To include in a direct and simple way all the contributions to the free energy coming from all the sites of the effective medium perturbed by the fluctuating site, the free energy $F(\xi_l)$ is calculated through the integration of its total derivative

$$\frac{\mathrm{d}F(\xi_l)}{\mathrm{d}\xi_l} = \frac{J}{2}(\xi_l - 2\langle \hat{S}_{lz}\rangle'_{\xi_l}), \tag{11}$$

instead of calculating it directly from a partition-function-like expression. The quantity $\langle \hat{S}_{lz}\rangle'_{\xi_l}$ in equations (9) and (11) is calculated as

$$\langle \hat{S}_{lz}\rangle'_{\xi_l} = \int_{-\infty}^{+\infty}\left(\sum_{\alpha\sigma}\sigma n_{l\alpha\sigma}(\varepsilon)\right) f(\varepsilon)\,\mathrm{d}\varepsilon, \tag{12}$$

where $f(\varepsilon)$ is the Fermi function and $n_{l\alpha\sigma}(\varepsilon)$ is the density of states (DOS) at the orbital $l\alpha\sigma$ of the system represented by the Hamiltonian $\hat{H}_{e+f} \equiv \hat{H}_{\mathrm{eff}} + \hat{\Gamma}_l$. In turn

$$\hat{\Gamma}_l = \sum_{\alpha\sigma}[U(\nu_l - \langle \nu_l \rangle) + \sigma J/2(\xi_l - \langle \xi_l \rangle)]\hat{n}_{l\alpha\sigma}.$$

Analogously, the quantity $\langle \hat{L}_{lz}\rangle'_{\xi_l}$ in equation (10) is calculated as

$$\langle \hat{L}_{lz}\rangle'_{\xi_l} = \int_{-\infty}^{+\infty}\left(\sum_{\sigma}\sum_{\alpha=-2}^{2}\alpha n_{l\alpha\sigma}(\varepsilon)\right) f(\varepsilon)\,\mathrm{d}\varepsilon. \tag{13}$$

The $n_{l\alpha\sigma}(\varepsilon)$ DOS appearing in equations (12) and (13) is obtained by using the known relation $n_{l\alpha\sigma}(\varepsilon) = -1/\pi\ \mathrm{Im}\{(\hat{G}_{e+f}(\varepsilon))_{l\alpha\sigma}\}$, where $(\hat{G}_{e+f}(\varepsilon))_{l\alpha\sigma}$ is the diagonal matrix element of the Green function for the system with Hamiltonian $\hat{H}_{e+f}$. Additionally, the Dyson equation is used to obtain $\hat{G}_{e+f}(\varepsilon)$ from $\hat{G}_{\mathrm{eff}}(\varepsilon)$ and $\hat{\Gamma}_l$. The matrix elements of $\hat{G}_{\mathrm{eff}}(\varepsilon)$ are calculated by using the Haydock–Heine–Kelly recursion method [23].

3. Results

Two bcc Fe slabs, (001) and (110), are considered for the calculations in this work. The slabs are modeled by employing Fe films thick enough for reaching the bulk behavior for zero and finite temperatures at their inner atomic layers. A thickness of 20 monolayers was observed to be enough for obtaining this behavior. In figure 1 we show a lateral cut for each one of the two slabs. All the atoms in planes parallel to the surface of the slabs are grouped in equivalent atom layers numbered with l and referenced as 'l layers' in this work. The $l = 1$ layer is the surface layer and l increases going into the slabs (see the figure). The density of atoms in figure 1 is adjusted to the same value in both (001) and (110) slabs, for appreciating in a clear way the differences in the local atomic environment between layers with the same l value in both slabs. To perform the calculations, the U, J and $t_{lm}^{\alpha\beta}$ parameters are determined for given values of the d electron number, SOC parameter and ground state bulk d band width, following a strategy similar to that used in a previous work involving ground state calculations [24]. Namely, we are using a d electron number of $n_{\mathrm{d}} = 7.2$, a spin–orbit coupling parameter of $\xi_{\mathrm{SOC}} = 0.05$ eV [8] and the $t_{lm}^{\alpha\beta}$ are taken as proportional to the Slater–Koster parameters (canonical values [25] varying as the inverse fifth power of the inter-atomic distance, $dd\sigma{:}dd\pi{:}dd\delta = -6{:}4{:}-1$) fitting a ground state d band width of $W_{db} = 6$ eV for Fe bcc bulk. The direct average Coulomb integral is taken as $U = W_{db}$ and the exchange average Coulomb integral as $J = 0.68$ eV. This value of J gives a total local moment of $\mu_{lz} = (2.09\mu_B)_{\mathrm{spin}} + (0.11\mu_B)_{\mathrm{orb}} = 2.2\mu_B$ at $T = 0$ for Fe bcc bulk.

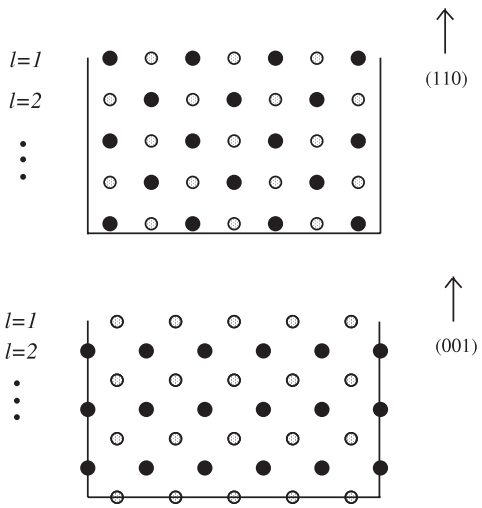

Figure 1. Lateral cuts for the (001) and (110) Fe slabs. The layers of equivalent atoms forming atomic planes parallel to the surface of the slabs are numbered with l. Atomic sites with different gray levels belong to different atomic planes parallel to the plane of the figure (transverse to the slabs' surface). The vector indicates the surface normal direction.

The spin and orbital local magnetizations are calculated along two different magnetization directions for each slab. For the case of the (001) [(110)] Fe slab, a first orientation of the spin and orbital z axes into the (001) [(110)] direction allows one to calculate the normal spin $M_{lz}(T)$ and orbital $L_{lz}(T)$ magnetizations. A second orientation of the spin and orbital z axes into the (100) [$(\bar{1}10)$] direction allows one to calculate the parallel spin $M_{lx}(T)$ and orbital $L_{lx}(T)$ magnetizations associated with this direction. Due to the fact that the values of $M_{lx}(T)$ differ from those of $M_{lz}(T)$ by at the most $1\times10^{-3}\mu_B$, they are not shown in this work. The results for the l =

7, 8, ... layers do not present significant differences to the eye in comparison with the results for the $l = 6$ layer, therefore they are not shown either.

3.1. (001) Fe slab results

The results for the temperature dependence of the spin and orbital local magnetizations for the (001) Fe slab are shown in figure 2. We discuss first the zero temperature limit for the results of the spin local magnetization found in figure 2(a). The surface layer ($l = 1$) has the biggest $M_{lz}(T \to 0)$ value in the figure, which is in total agreement with the fact that the atomic sites forming this layer are the least inter-atomically connected in the system and, therefore, are the ones having the largest tendency to localize electrons (band narrowing) and to accumulate spin moment at $T \to 0$ (Stoner criteria). On the other hand, as the spin polarization can be electronically induced from one atomic region to another in an itinerant system, we should expect the relatively large $T \to 0$ spin magnetization at the $l = 1$ layer to induce, when we go from $l = 1$ to 6, a simple decreasing behavior towards the ground state bulk value in $M_{lz}(T \to 0)$. However, a decreasing sequence of values is only observed from $l = 1$ to 3. At the $l = 4$ layer we observe that $M_{lz}(T \to 0)$ increases and that, after this layer, it starts a damped-like oscillation towards the ground state bulk value with l. This behavior is related to small charge transfers occurring at the superficial region of the slab and, specifically, to a slight band broadening occurring at the $l = 2$ and 3 layers. It is worth mentioning that all the obtained results for the spin local magnetization at $T \to 0$ are in good agreement with calculations performed independently by ourselves at $T = 0$ within the same model (as we will show in section 3.3, this is not trivial). Moreover, the physical explanations given here about the layer distribution of the spin magnetic local magnetization at $T \to 0$ coincide with those given in numerous works involving ground state calculations for low dimensional TM systems [26] within the same model. In this sense, we observe the $T \to 0$ limit of the obtained results for $M_{lz}(T)$ to be correct.

Recall that the atomic sites forming the surface layer ($l = 1$) are the least inter-atomically connected in the (001) Fe slab. This implies, besides the fact that this layer accumulates the biggest spin local magnetic moments in the system at $T \to 0$, that this layer also has the lowest magnetic stability level against thermal fluctuations in the system (less ferromagnetic inter-atomic couplings for a site of the layer). This is clearly observed in figure 2(a): the $M_{lz}(T)$ curve for $l = 1$ goes to zero with temperature faster than all the other spin magnetization curves and even crosses them all but the $l = 3$ spin magnetization curve. In turn, the relative low ferromagnetic stability at the surface layer ($l = 1$) should also weaken the resistance against thermal fluctuations on the ferromagnetism of the neighboring l layers. Therefore, the $M_{lz}(T)$ curve for $l = 2$ and 3 should go to zero with temperature more quickly than the curves for $l = 4, 5$ and 6. However, the spin magnetization curve for the $l = 2$ layer is observed to go to zero at the lowest rate with temperature in figure 2(a). An analysis of the $F(\xi_l)$ curves for the six

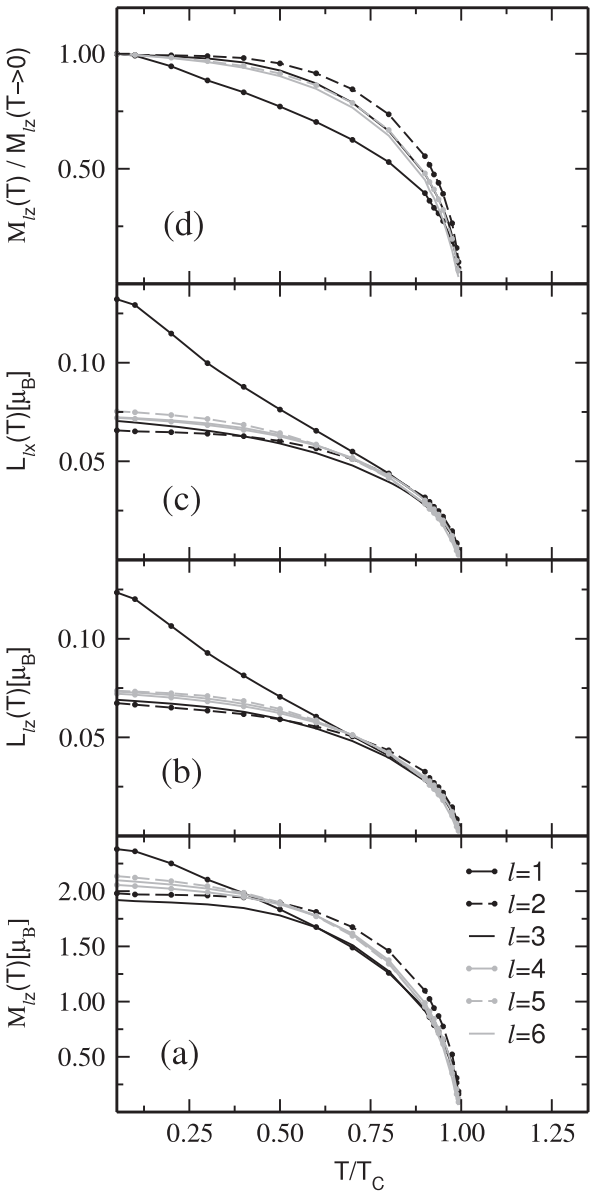

Figure 2. Temperature dependence of the spin and orbital local magnetizations calculated along the z [(001)] and x [(100)] directions of the (001) Fe bcc slab. The results are given only for the six first atomic layers defined in figure 1. We have in (a) the spin results, in (b) the orbital results for the z direction, in (c) the orbital results for the x direction and in (d) the spin results normalized with the corresponding ground state limit value.

first l layers of the slab indicates that the atoms of the $l = 1$ layer have a tendency to an antiferromagnetic coupling with their neighboring atoms, including those of the same $l = 1$ layer (see the next paragraph). This tendency diminishes with temperature at the same time as the spin local magnetization and this is the cause for the low decaying rate with temperature observed for the spin magnetization at the $l = 2$ layer. Although, in a very weak way, the $l = 3$ layer presents basically the same behavior in the spin magnetization as the $l = 2$ layer (see figure 2(d)). For the remaining $l = 4, 5$ and 6 layers, the local spin magnetization decreases with temperature at a very similar rate, almost the bulk's rate.

In order to clarify the relatively slow decaying with temperature of the local magnetization at the $l = 2$ layer of the (001) slab (related to the tendency to antiferromagnetic coupling mentioned in the previous paragraph), it is necessary to perform an additional analysis on the temperature dependence of the free energy $F(\xi_l)$ for its neighboring $l = 1$ layer. Figure 3 shows the results for the free energy change $\Delta F(\xi_l) \equiv F(\xi_l) - F(\xi_l^+)$ associated with the fluctuations of the exchange field ξ_l at the surface $l = 1$ layer, where ξ_l^+ denotes the position of the minimum of the free energy for $\xi_l > 0$. The results are presented for several representative reduced temperatures $t = T/T_C$. From the figure, we observe the existence of two well defined minima $F(\xi_l^-)$ and $F(\xi_l^+)$ located at $\xi_l < 0$ and $\xi_l > 0$, respectively, for every t value on the figure. The position of these two minima stays approximately fixed when the temperature changes, which indicates that the $\xi_{l=1}$ local exchange field fluctuates keeping an approximately constant modulus. We also observe from the figure a nonmonotonous behavior with temperature of the free energy change $\Delta F(\xi_l^-) = F(\xi_l^-) - F(\xi_l^+)$ required for flipping the exchange field from ξ_l^+ to ξ_l^-. This flipping free energy change has a relative small value at $T \to 0$, increases with temperature reaching a maximum value at $t = 0.6$ and decreases, as physically expected, when we approach $t = 1$ (the Curie temperature). The fact that $\Delta F(\xi_l^-)$ has a relatively small value and that it first increases with temperature for relatively low temperatures indicates a tendency to antiferromagnetism of an electronic origin at the surface $l = 1$ layer, which is decreasing in strength with temperature. Notice that a behavior not showing this tendency to antiferromagnetic coupling would be one where the free energy change does not have a relatively small value at low temperature and decreases monotonously with temperature until the Curie temperature is reached. Finally, this tendency to antiferromagnetism can not be obtained by using solid local magnetic moment models with fixed interatomic ferromagnetic coupling, as for example, by using the Heisenberg model.

By orientating the spin and orbital z axes into the (001) direction, we calculate the orbital local magnetization for the z [(001)] direction of the slab. The results are shown in figure 2(b). We observe from the figure that when we go from the surface $l = 1$ layer to the $l = 2$ layer, $L_{lz}(T \to 0)$ quickly decreases to almost its ground state bulk value, having a drop of nearly 50% in the value of the orbital moment. Additionally, we observe that, although not in a proportional way, the variation of $L_{lz}(T \to 0)$ with l roughly follows the observed trend for $M_{lz}(T \to 0)$ in figure 2(a). The local narrowing or broadening of the d band coming from the change in the local atomic environment affect both spin and orbital magnetizations[5]. However, this occurs in a weaker way for the orbital magnetization because of the small intensity of the SOC interaction. By orientating the spin and orbital z axes into the (100) direction, we calculate the local orbital magnetization

[5] As it is known, the orbital magnetization at zero temperature in the d band model is generated mostly in the minority spin band by the orbital unfolding caused by the SOC interaction; its magnitude is determined by the height of the DOS at the Fermi level.

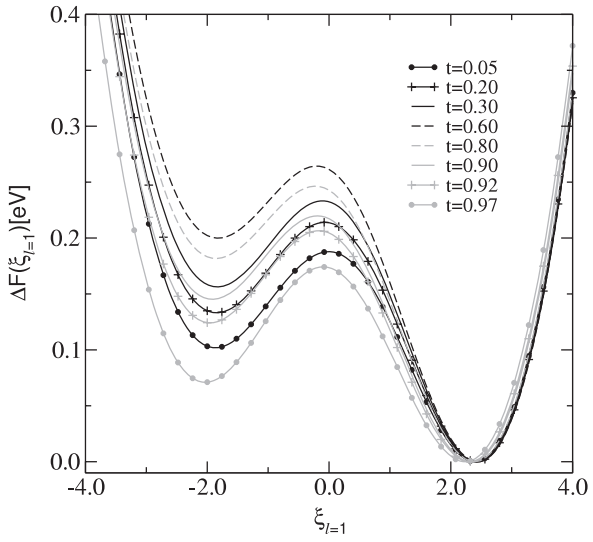

Figure 3. Dependence on the reduced temperature $t = T/T_C$ of the $\Delta F(\xi_l) \equiv F(\xi_l) - F(\xi_l^+)$ free energy associated to the exchange fluctuations of ξ_l at the surface $l = 1$ layer, where ξ_l^+ denotes the position of the minimum of the free energy for $\xi_l > 0$.

for the x [(100)] direction of the slab. The results are shown in figure 2(c). We notice that at the surface $l = 1$ layer, $L_{lx}(T \to 0)$ is slightly greater than $L_{lz}(T \to 0)$, this is due to the local anisotropy in the atomic environment existing there. A detailed explanation for this magnetic anisotropy effect relies on the characteristic atomic environment at the surface layer of the system and on the specific d band filling of a Fe system[6]. Moreover, $L_{lx}(T \to 0)$ is immediately reduced to approximately the ground state bulk value when we go from the superficial $l = 1$ layer to the $l = 2$ layer and, in general, its behavior with l roughly follows that of $M_{lz}(T \to 0)$. However, the anisotropy between the z and x magnetization directions observed at the $l = 1$ layer is not clearly preserved in the rest of the l layers. This is due to the specific form of the local DOS around the Fermi energy level preventing a possible induction of magnetic anisotropy from the $l = 1$ to the rest of the layers. As for the case of the $T \to 0$ spin results, the obtained results for the orbital magnetization at $T \to 0$ are in good agreement with $T = 0$ calculations performed independently by ourselves within the same model. Besides the physical explanations given here, these kind of results are well known and discussed in many ground state theoretical works found in the literature and performed for related TM systems, as for example thin films [27].

For the same l value, the $L_{lz}(T)$ and $L_{lx}(T)$ curves in figures 2(b) and (c) do not show significant differences from each other at finite temperature. The few slight observed differences between both magnetization curves come from the $T \to 0$ anisotropy effects mentioned in the last paragraph. As

[6] The local atomic environment in the surface layer causes a small delocalization in the electronic states with orbital angular moment normal to the surface. A larger value of orbital moment implies a larger delocalization. At the same time, the opposite occurs for states with orbital angular moment parallel to the surface. This delocalization and the characteristic d band filling of Fe (around the half filling of the minority band) causes the normal angular moment atomic states to average for less magnetization than the parallel ones.

the temperature rises from zero, the orbital local magnetization at every l layer of the slab decreases together with the spin local magnetization, reaching a zero value at the Curie temperature (T_C). In a general way, the shape of the orbital magnetization curves in figures 2(b) and (c) resembles that of the spin magnetization ones in figure 2(a). Geometrical aspects such as the slope and concavity of a given orbital magnetization curve are similar to those of the corresponding spin magnetization curve. For instance, the orbital magnetization curve for the surface $l = 1$ layer has an approximately linear trend at low and intermediate temperatures in the interval $[0, T_C]$, just like the one appearing in the corresponding spin magnetization curve. This resemblance of the orbital magnetization curves to the spin magnetization curves comes from the property of the SOC interaction generating a small orbital unfolding of every spin state occurring at finite temperature. As the temperature rises from zero, spin excited states appear in the system, bringing with them configurations of small but non-zero orbital polarization different to that of the spin ground state. For low temperatures, positive spin states with exchange values smaller than that of the spin ground state play the key role in the system and, therefore, the average orbital polarization decreases with temperature, mainly because the orbital contribution of these spin states is smaller than that of the spin ground state. For high temperatures, negative spin states appear in the system bringing with them orbital contributions that cancel those of the positive spin states. Finally, at the Curie temperature, a full canceling occurs for both orbital and spin polarizations.

The Curie temperature value obtained with our approach ($T_C \approx 2000$ K) is comparable with other reported values in the literature involving first principles calculations, electron correlation effects and/or more sophisticated mean field approaches [12, 14]. However, this value is appreciably larger than the experimental one of $T_C^{exper} \approx 1043$ K. The inclusion in our approach of a more sophisticated mean field theory, additional spin excitations like spin-waves, non-collinear moments, short-range magnetic order effects or/and electronic correlations beyond the static approximation, should tend to reduce our T_C value, improving in this way the quantitative agreement between the calculated and the experimental value.

3.2. (110) Fe slab results

The local atomic environment at the superficial region of the (110) Fe slab is qualitatively different to that of the (001) Fe slab. For the (110) Fe slab, the nearest neighbor (NN) distance occurs between atoms of adjacent l layers and between atoms of the same l layer. On the other hand, for the (001) Fe slab, the NN distance occurs only between atoms of adjacent l layers. This implies that at the superficial region of the (110) Fe slab, the electronic itinerancy occurring between atoms of the same l layer is as important as those occurring between adjacent l layers whereas, for the case of the (001) Fe slab, the itinerancy occurring between adjacent l layers is the most important. In the particular case of the surface $l = 1$ layer, one can anticipate that the level of electronic itinerancy at this layer for the case of the (001) slab is going to be lower than for the case of the (110) slab.

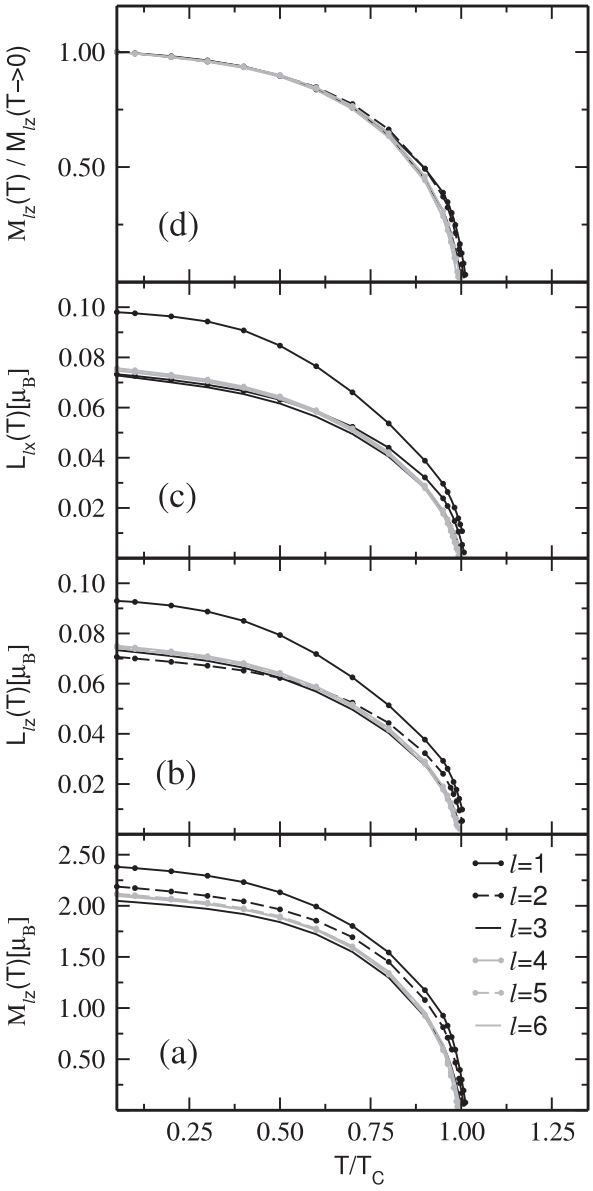

Figure 4. Temperature dependence of the spin and orbital local magnetizations calculated along the z [(110)] and x [$(\bar{1}10)$] directions of the (110) Fe bcc slab. The results are given only for the six first atomic layers defined in figure 1. We have in (a) the spin results, in (b) the orbital results for the z direction, in (c) the orbital results for the x direction and in (d) the spin results normalized with the corresponding ground state limit value.

Figure 4 shows the results for the temperature dependence of the spin and orbital local magnetizations for the z [(110)] and x [$(bar110)$] directions of the (110) Fe slab. Figure 4(a) contains the spin, figures 4(b) and (c) the orbital and figure 4(d) the normalized spin magnetization results. We observe in figure 4(a) that the ground state limit of the spin local magnetization behaves in a very similar way with l to that observed in the (001) Fe slab case: it decreases when we go from $l = 1$ to 3 and then increases again when we go from $l = 3$ to 4. As for the (001) slab, small charge transfers occur in such a way that for this slab we do not observe a simple decreasing behavior with l in $M_{lz}(T \to 0)$. In spite of this

similar behavior, there is a systematic qualitative difference between the (110) and (001) spin ground state limits. The change of $M_{lz}(T \rightarrow 0)$ between adjacent l layers is, in general, smaller than in the (001) case and, unlike this last case, the ground state Fe bcc bulk value is practically reached at the $l = 4$ layer. In general, the deviation with respect to the ground state bulk behavior in the superficial region of the (110) Fe slab is smaller than in the superficial region of the (001) Fe slab. This is due to the difference between the atomic environment in the superficial region of the two slabs. At finite temperature, we also notice that the spin magnetization curves change with l in a smoother way than in the (001) case (see figure 4(a)). For instance, the $M_{lz}(T)$ curve for the surface layer ($l = 1$) does not have the linear trend observed in the case of the (001) slab, because the inter-atomic connectivity in this layer is not low enough to cause this behavior; even so, the decaying rate with temperature of the spin local magnetization in the $l = 1$ layer is found to be larger than in the bulk-like $l = 4, 5, 6$ layers for low and intermediate temperatures in $[0, T_C]$. Another difference, with respect to the (001) slab results, is the fact that the spin magnetization curve for the $l = 2$ layer does not go to zero with temperature in a slower way than for the remaining layers in figure 4(a). The effect of slow decaying with temperature of the magnetization occurs in the $l = 3$ layer, although in a weaker way. The small charge transfers occurring in this case are not strong enough for creating, with the same intensity, the tendency to antiferromagnetism observed in the $l = 1$ layer of the (001) Fe slab.

The orbital local magnetization results for the (110) Fe slab are shown in figures 4(b) and (c). Figure 4(b) contains the results for the magnetization direction along z and figure 4(c) the results for the magnetization direction along x. The l dependence in figure for $L_{lx}(T \rightarrow 0)$ and $L_{lz}(T \rightarrow 0)$ follows roughly that already observed for $M_{lz}(T \rightarrow 0)$ and, as also observed for those $M_{lz}(T \rightarrow 0)$ results, the change of $L_{lx}(T \rightarrow 0)$ and $L_{lz}(T \rightarrow 0)$ between adjacent l layers is smaller than in the case of the (001) slab, due to the difference between the atomic environment in the superficial region of the two slabs. The anisotropy effect $L_{lx}(T \rightarrow 0) > L_{lz}(T \rightarrow 0)$ occurring in the surface $l = 1$ layer is also observed to be less significant that in the (001) case. Lastly, at finite temperature, the shape of each orbital local magnetization curve resembles that of its corresponding spin local magnetization. For instance, the lack of a linear trend with temperature on the $M_{lz}(T)$ curve for the surface $l = 1$ layer also happens in the corresponding $L_{lx}(T)$ and $L_{lz}(T)$ curves.

3.3. Varying the d band filling and performing geometrical relaxations

The results obtained at this point in this work reflect the structural characteristics of the studied systems very well. However, there are several points related to the results which need to be addressed. The most important one is the fact that in the experimental results of Pfandzelter *et al* one observes a gradual transition in the temperature dependence of the local magnetization when one goes into the internal region of the slab. In particular, the observed trend in our calculation for the temperature dependence of the magnetization in the $l = 2$ layer ((001) slab) is not observed in the corresponding experimental result. By reviewing the $T \rightarrow 0$ limit of our results and additional ground state calculations, we arrive at the conclusion that, in the first instance, structural relaxations are required in the calculations. Due to limitations in computational time and in the theory used, a convenient scheme for performing these structural relaxations is to initially carry out systematic modifications at zero temperature on the inter-l-layer distances in the non-bulk region of the slabs. Then, the observed qualitative changes in the $M_{lz}(T = 0)$ values could indicate sets of structural configurations defined by a similar qualitative behavior in the temperature dependence of the local magnetization. This will help us to reduce the number of structural configurations to be explored at finite temperature when we search for the required experimental behavior. It is worth mentioning that due to the nature of the model used, here we do not have the option of performing standard geometrical relaxations ruled by energy considerations as in the case of first principle calculations. Even more, we also can not directly take structural parameters coming from ground state first principle optimizations for our calculations, because of the natural differences between first principle Hamiltonians and our used model. These reasons lead us to perform a relaxation process consisting of finding correct parameters for the model which give the observed experimental trends on temperature for magnetic properties. In spite of this, we start the relaxation process taking into account results coming from ground state first principle calculations existing in the literature.

The variation on the inter-l-layer distances for the ground state structural relaxations is kept in the range of $\pm 10\%$ of the corresponding bulk inter-layer value. The relaxations are performed only for the (001) slab and carried out following existing experimental and theoretical relaxation results [28]. The first goal in the relaxation process was to find a configuration for the inter-l-layer distances which led to a decreasing trend in $M_{lz}(T = 0)$ for increasing l (going into the slab), thinking this could help in obtaining the required experimental behavior in our results. The variation of only two of the first inter-l-layer distances was enough to get the desired behavior in $M_{lz}(T = 0)$. It was obtained for values of inter-l-layer distances that represent, first, contractions of approximately above 5% (with respect to the corresponding bulk inter-layer value) on the inter-layer distance between the $l = 1$ and the $l = 2$ layers and, second, expansions of approximately above 6% on the inter-layer distance between the $l = 2$ and 3 layers. After having found them, finite temperature calculations for only the spin magnetization (SOC interaction switched off) were performed for several inter-l-layer distances around these values and also around the non-relaxed values. As expected, the finite temperature calculations around the relaxed values show results with a behavior qualitatively similar to those of the non-relaxed situation. However, the finite temperature calculations around the relaxed values present a problem. They have the apparent flaw of not reducing to our mentioned independently performed ground state calculations when $T \rightarrow 0$. The apparent

flaw is mainly observed in the superficial layer of the slab. Antiferromagnetic-like instabilities, possibly related to the tendency to antiferromagnetic behavior already observed in the previous sections of this work, play a key role by diminishing the limit values $M_{lz}(T \rightarrow 0)$ with respect to those of our independently performed ground state calculations.

The antiferromagnetic behavior in the d band model is generally associated with low d band filling effects. Depending on the system under study, the antiferromagnetic behavior predicted by this model can be considered correct or incorrect. For TM systems with a d band filling close to the half band filling, one expects results showing an antiferromagnetic behavior to be correct whereas, for TM systems with a d band filling close to the full band filling, such behavior is expected to be incorrect. For TM systems between these two extreme cases, a scan of the d band filling is always necessary to take into account all possible physical results. On the other hand, it is known that the *s* and/or *p* electronic bands with bare energy levels above those of the d band in a TM system help to reduce, or to eliminate, weak antiferromagnetic behaviors. Therefore, its inclusion sometimes becomes necessary for the calculations. However, most of the time, some d–sp hybridization and sp band filling effects can be emulated by slightly increasing the d band filling in the d band model (the direct Coulomb and exchange interactions associated with the involved sp electrons generally do not play an important role for the magnetism). If this is the case, a possible extension to a spd band model can be avoided. Taking into account these considerations, we decided that the correct approach for reproducing the observed finite temperature experimental behavior must include d band filling variations in the calculations. Despite the resulting approach turning out to be relatively slow, the expected finite temperature results are straightforwardly obtained, at least approximately for the first four l layers. For a d band filling of about 7.4, the disagreement of the limit values $M_{lz}(T \rightarrow 0)$ with our independently calculated ground state calculations disappears and, in this way, we obtain finite temperature results more similar to the experimental ones.

Figure 5 shows structurally relaxed representative results for the temperature dependence of the spin and orbital magnetization (SOC interaction switched on) calculated along the z [(001)] and x [(100)] directions of the (001) slab. The values for the corresponding inter-l-layer distances mean a contraction of ∼5% on the first inter-layer distance ($l = 1$ and 2) and an expansion of ∼5% on the second one ($l = 2$ and 3). The used d band filling is also modified to $n_{\mathrm{d}} = 7.4$. For this new value of n_{d}, the value for the exchange average integral J has been slightly increased to again fit a total local moment of $\mu_{lz} = 2.2\mu_{\mathrm{B}}$ at $T = 0$ for the bulk. Figure 5(a) shows the results for the temperature dependence of the spin local magnetization on the z direction $M_{lz}(T)$ as obtained from equation (9) and figure 5(d) shows these same results but normalized as $M_{lz}(T)/M_{lz}(T \rightarrow 0)$. We first notice in figure 5(a) the achievement in getting a decreasing behavior as a function of l in $M_{lz}(T \rightarrow 0)$, albeit the changes from $l = 1$ to 2 and from $l = 5$ to 6 are not very evident to the eye. It was checked that our independently calculated ground state values are recovered from the $M_{lz}(T)$ values when $T \rightarrow 0$. On the other hand, for finite temperatures we observe in the figure that the temperature dependence of the spin magnetization is becoming qualitatively similar to the experimental one, at least for the first four l layers. For instance, the decreasing with temperature of the local magnetization in the $l = 2$ layer is now slightly slower than that in the $l = 1$ layer and also slightly faster than that in the $l = 3$ layer. The $M_{lz}(T)/M_{lz}(T \rightarrow 0)$ curves displayed in figure 5(d) show in a clearer way, the fact

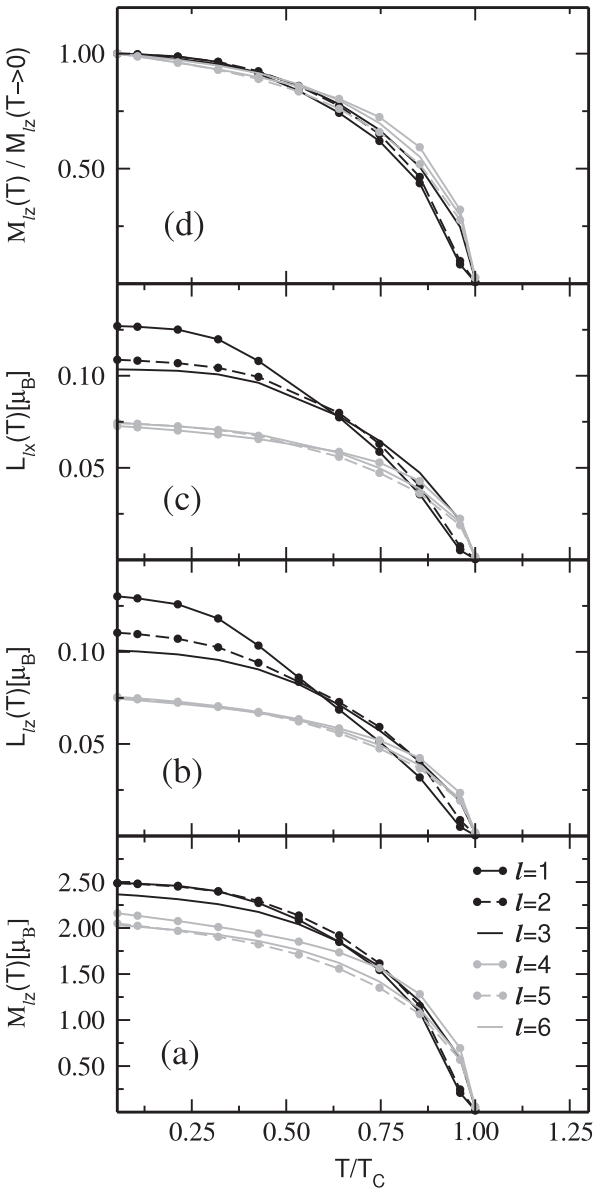

Figure 5. Temperature dependence of the spin magnetization calculated along the z [(001)] and x [(100)] directions of the (001) slab. The results are representative and include a structural relaxation and a variation of the d band filling. The inter-l-layer spacing and d band filling values used for the calculations are indicated in the text. The thickness of the film modeling the slab is 10 monolayers. We have in (a) the results for the temperature dependence of the spin local magnetization on the z direction $M_{lz}(T)$, in (b) those for the orbital local magnetization in the z direction $L_{lz}(T)$, in (c) those for the orbital local magnetization in the x direction $L_{lx}(T)$ and in (d) the same results as in (a) but normalized as $M_{lz}(T)/M_{lz}(T \rightarrow 0)$.

that the behavior of the spin local magnetization as a function of the temperature changes gradually to bulk-like when we go into the slab, at least for the first four l layers. Finally, for the results for the orbital magnetization on figures 5(b) and (c), we can observe that all the observed properties for the non-relaxed and $n_d = 7.2$ situations are recovered. From all the previous observations, we have the following preliminary conclusion: the itinerant nature of the magnetism of TM systems, the main characteristic of the d band model, generates a very complex dependence of the ground state and finite temperature magnetism on the geometrical structure of the slabs and d band filling. Further geometrical relaxations, which would include a change on inter-l-layers distances beyond the ones already taken into account in this work, are necessary for recovering in a better way the experimental behavior.

4. Summary and conclusions

Our work reports for the first time, to the best of our knowledge, calculations for the temperature dependence of the orbital local magnetization in the superficial region of a ferromagnetic TM system. The temperature dependence of the spin and orbital magnetizations has been calculated for two Fe slab systems presenting different local atomic environments between them in their superficial region. The calculations were performed in the framework of an electronic d band model which is known to reproduce well the interplay between the local atomic environment and electronic itinerancy at zero temperature. The spin and charge thermal fluctuations are treated within the static approximation and a simple mean field approach, which allows us to perform the calculations in feasible computational times. An acceptable clear complex dependence on the local atomic environment and d band filling is observed for the ground state and finite temperature local magnetization in the superficial region of the slabs. The complexity of this dependence can not be predicted in a direct way by Heisenberg-like models of localized atomic moments. This is clearly understood because in the case of an electronic itinerant model this coupling is the result of the electronic properties of the system whereas, in models of localized atomic moments, the inter-atomic magnetic coupling enters generally as a parameter.

As a starting configuration, the interplanar atomic distances in the superficial region of the slabs were taken as equal to the bulk system. For this case, the zero temperature limit of the local orbital and spin magnetization was observed to match very well with ground state results independently calculated by ourselves. Furthermore, a well known characteristic physical behavior related to the effects of electronic localization on the spin and orbital local magnetizations in the superficial atomic layers of the slabs was observed in the results for the $T \to 0$ limit. Moreover, well known characteristic anisotropy effects on the $T \to 0$ limit of the orbital local magnetization in these layers were also observed in our calculations. On the other hand, at finite temperatures, the local spin magnetization was observed to agree only in a partial way with experimental results. With the goal of recovering in a more complete way this agreement between experimental and theoretical results, modifications to the original superficial interplanar atomic distances were performed. However, these modifications brought up the apparent flaw of mismatching the zero temperature limit of the local spin magnetization with our independently calculated ground state results. This apparent flaw is related to a tendency to antiferromagnetism of electronic origins observed in the most superficial atomic layers of the slabs. The tendency to antiferromagnetism was reduced by increasing, by a small quantity, the d band filling value on the systems and, in this way, the calculated results took a form qualitatively more approximating to the experimental ones.

In a general way, the temperature dependence of the orbital local magnetization is observed to follow the same trend as the spin local magnetization, with some slight differences. For instance, the approach to bulk-like behavior when we go into the internal region of the slabs is faster in the orbital case for both ground state and finite temperature results.

Finally, we consider that some extensions to the used theory and mean field approach would certainly be desirable for quantitatively improving our results. For instance, the inclusion of non-collinear spin fluctuations and the use of more sophisticated mean field approaches would be desirable to obtain a Curie temperature value closer to the experimental one.

Acknowledgments

Computer resources were provided by CNS (IPICyT, México) and by ACARUS (UNISON, México). This work was supported by CONACYT through grants CONACYT 2005-J48897-Y (MRR). RGA acknowledges support from PROMEP, México.

References

[1] Gambardella P, Rusponi S, Veronesse M, Dhesi S S, Grazioli C, Dallmeyer A, Cabria I, Zeller R, Dederich P H, Kern K, Carbone C and Brune H 2003 *Science* **300** 1130
Skumryev V, Stoyanov S, Zhang Y, Hadjipanayis G, Givord D and Nogues J 2003 *Nature* **423** 850
Sun S, Murray C B, Weller D, Folks L and Moser A 2000 *Science* **287** 1989
Prandolini M J, Manzhur Y, Weber A, Potzger K, Bertschat H H, Ueno H, Miyoshi H and Dietrich M 2004 *Appl. Phys. Lett.* **85** 76
Grimsditch M, Hoffmann A, Vavassori P, Shi H and Lederman D 2003 *Phys. Rev. Lett.* **90** 257201
Chung S H, Hoffmann A and Grimsditch M 2005 *Phys. Rev.* B **71** 214430
[2] Abraham D L and Hopster H 1987 *Phys. Rev. Lett.* **58** 1352
[3] von der Linden W, Donath M and Dose V 1993 *Phys. Rev. Lett.* **71** 899
[4] Sirotti F, Panaccione G and Rossi G 1995 *Phys. Rev.* B **52** R17063
[5] Pfandzelter R and Potthoff M 2001 *Phys. Rev.* B **64** 140405(R)
[6] Kisker E, Schröder K, Gudat W and Campagna M 1985 *Phys. Rev.* B **31** 329
Kirschner J, Glöbl M, Dose V and Scheidt H 1984 *Phys. Rev. Lett.* **53** 612
Kirschner J 1984 *Phys. Rev.* B **30** 415

[7] Pfandzelter R, Winter H, Urazgil'din I and Rösler M 2003 *Phys. Rev.* B **68** 165415
Pfandzelter R, Bernhard T and Winter H 2003 *Phys. Rev. Lett.* **90** 036102
Gruyters M, Bernhard T and Winter H 2005 *Phys. Rev. Lett.* **94** 227205
[8] Bruno P 1989 *Phys. Rev.* B **39** 865
[9] Pastor G M, Dorantes-Dávila J, Pick S and Dreyssé H 1995 *Phys. Rev. Lett.* **75** 326
Dorantes-Dávila J and Pastor G M 2005 *Phys. Rev.* B **72** 085427
Galanakis I, Alouani M and Dreyssé H 2000 *Phys. Rev.* B **62** 3923
Brown G, Kraczek B, Janotti A, Schulthess T C, Stocks G M and Johnson D D 2003 *Phys. Rev.* B **68** 052405
[10] Herrmann T, Potthoff M and Nolting W 1998 *Phys. Rev.* B **58** 831
Wu J H, Chen H Y and Nolting W 2001 *Phys. Rev.* B **65** 014424
Mryasov O N, Nowak U, Guslienko K Y and Chantrell R W 2005 *Europhys. Lett.* **69** 805
Staunton J B, Ostanin S, Razee S S A, Gyorffy B L, Szunyogh L, Ginatempo B and Bruno E 2004 *Phys. Rev. Lett.* **93** 257204
[11] Gutzwiller M C 1965 *Phys. Rev.* **137** A1726
[12] Lichtenstein A I, Katsnelson M I and Kotliar G 2001 *Phys. Rev. Lett.* **87** 067205
[13] Hubbard J 1979 *Phys. Rev.* B **19** 2626
Hubbard J 1979 *Phys. Rev.* B **20** 4584
Hasegawa H 1980 *J. Phys. Soc. Japan* **49** 178
Hasegawa H 1980 *Phys. Rev.* B **49** 963
[14] Garibay-Alonso R, Dorantes-Dávila J and Pastor G M 2006 *Phys. Rev.* B **73** 224429
[15] Garibay-Alonso R, Villaseñor-González P, Dorantes-Dávila J and Pastor G M 2004 *J. Phys.: Condens. Matter* **16** S2257
Garibay-Alonso R, Dorantes-Dávila J and Pastor G M 2002 *J. Appl. Phys.* **91** 8254
[16] Pick S and Dreyssé H 1993 *Phys. Rev.* B **48** 13588
Pastor G M, Dorantes-Dávila J, Pick S and Dreyssé H 1995 *Phys. Rev. Lett.* **75** 326
[17] See for example Dorantes-Davila J, Vega A and Pastor G M 1993 *Phys. Rev.* B **47** 12995
Vega A, Dorantes-Dávila J, Balbás L C and Pastor G M 1993 *Phys. Rev.* B **47** 4742 and references therein
[18] See for example Bruus H and Flensberg K 2009 *Many-Body Quantum Theory in Condensed Matter Physics: An Introduction* (New York: Oxford University Press) p 16
[19] Pastor G M, Dorantes-Dávila J and Bennemann K H 2004 *Phys. Rev.* B **70** 064420
[20] Garibay-Alonso R, Dorantes-Dávila J and Pastor G M 2009 *Phys. Rev.* B **79** 134401
[21] Fulde P 1991 *Electron Correlations in Molecules and Solids* (*Springer Series in Solid State Sciences*) (Berlin: Springer)
[22] Economou E N 1983 *Green's Functions in Quantum Physics* (*Springer Series in Solid State Sciences* vol 7) (Heidelberg: Springer)
[23] Haydock R 1980 *Solid State Physics* vol 35, ed H Ehreinreich, F Seitz and D Turnbull (New York: Academic) p 215
[24] Garibay-Alonso R and López-Sandoval R 2005 *Solid State Commun.* **134** 503
[25] Moruzzi V L and Marcus P M 1988 *Phys. Rev.* B **38** 1613
Harrison W A 1983 *Phys. Rev.* B **27** 3592
Heine V 1976 *Phys. Rev.* **153** 673
[26] Rodríguez-López J L, Dorantes-Dávila J and Pastor G M 1998 *Phys. Rev.* B **57** 1040
Dorantes-Dávila J, Dreyssé H and Pastor G M 1997 *Phys. Rev.* B **55** 15033
Tsujikawa M, Hosokawa A and Oda T 2008 *Phys. Rev.* B **77** 054413
[27] Dunn J H, Arvanitis D and Mårtensson N 1996 *Phys. Rev.* B **54** 11157(R)
Tischer M, Hjortstam O, Arvanitis D, Dunn J H, May F, Baberschke K, Trygg J, Wills J M, Johansson B and Eriksson O 1995 *Phys. Rev. Lett.* **75** 1602
Thiele J, Boeglin C, Hricovini K and Chevrier F 1996 *Phys. Rev.* B **53** R11934
[28] Escaño M C, Nakanishi H and Kasai H 2207 *J. Phys.: Condens. Matter* **19** 482002
Leibbrandt G W R, van Wijk R and Habraken F H P M 1993 *Phys. Rev.* B **47** 6630
Wang Q, Li Y S, Jona F and Marcus P M 1987 *Solid State Commun.* **61** 12933
Ohnishi S, Weinert M and Freeman A J 1984 *Phys. Rev.* B **30** 36